

# Supporting Information for ”Remote sensing retrieval of isoprene concentrations in the Southern Ocean”

Pablo Rodríguez-Ros<sup>1</sup>, Martí Galí<sup>2</sup>, Pau Cortés<sup>1</sup>, Charlotte Mary Robinson<sup>3</sup>,

David Antoine<sup>3,4</sup>, Charel Wohl<sup>5</sup>, MingXi Yang<sup>5</sup>, Rafel Simó<sup>1</sup>

<sup>1</sup>Institut de Cincies del Mar, ICM-CSIC, Passeig Marítim de la Barceloneta, 37-49, 08003, Barcelona, Catalonia, Spain

<sup>2</sup>Earth Sciences Dept, Barcelona Supercomputing Center (BSC-CNS), Barcelona, Catalonia, Spain

<sup>3</sup>Remote Sensing and Satellite Research Group, School of Earth and Planetary Sciences, Curtin University, Perth, Australia

<sup>4</sup>Sorbonne Université, CNRS, Laboratoire d’Océanographie de Villefranche, LOV, F-06230 Villefranche-sur-Mer, France

<sup>5</sup>Plymouth Marine Laboratory, Plymouth, United Kingdom

## Contents of this file

1. Tables S1 and S2
2. Figures S1 to S5

## Introduction

This document contains tables and figures that are not essential to the main text but provide valuable and additional or complementary information of the data analysis. All these supplementary tables and figures are cited in the main text.

---

- Table S1 provides basic information of the cruises where data have been taken from, with average and ranges of the observed isoprene concentrations, the broad regional coverage, and the isoprene analysis method used.
- Table S2 lists the remote sensing variables used: source, reprocessing status, mean and range.
- Figure S1 describes the frequency distribution of isoprene observations over the solar day. This demonstrates that the dataset used in this work is not heavily biased to any period of the day, although samples around noon are slightly more abundant. This remarkably even distribution is probably due to the fact that a large proportion of the database is contributed by automated instruments or underway measurements at high temporal resolution (ANDREXII, KH-09-5, part of PEGASO).
- Figure S2 displays the results of the Redundancy Analysis performed for isoprene measurements and the remote sensed variables (see Table S2 for abbreviations).
- Figure S3 illustrates how ISOREMS predicts the observations used for its development ( $n = 327$ ), as well as how ISOREMS residuals relate to other remote sensing variables not used in the algorithm. The plots indicate that no variable other than CHL and SST improve significantly isoprene prediction. Moreover, they do not show any evidence for nonlinear relationships performing better than linear regressions.
- Figure S4 illustrates the skills and uncertainty of ISOREMS predictions assessed using a random sampling method for validation, as explained in the main text.
- Figure S5 shows the monthly climatology of isoprene emission fluxes calculated from ISOREMS-predicted isoprene concentrations and climatologies of wind speed and SST

(details are given in the main text). This figure is not included in the main text because it is a secondary or derived product of ISOREMS, which has been developed to directly predict surface ocean concentrations. These emission flux fields, combined with several assumptions explained in the main text, are used to calculate the monthly and annual integrated regional isoprene emissions shown in Figure 3.

## References

- Hackenberg, S., Andrews, S., Airs, R., Arnold, S., Bouman, H., Brewin, R., ... others (2017). Potential controls of isoprene in the surface ocean. *Global Biogeochemical Cycles*, 31(4), 644–662. doi: <https://doi.org/10.1002/2016GB005531>
- Holte, J., Talley, L. D., Gilson, J., & Roemmich, D. (2017). An argo mixed layer climatology and database. *Geophysical Research Letters*. doi: <https://doi.org/10.1002/2017GL073426>
- Legendre, P., & Legendre, L. F. (2012). *Numerical ecology*. Elsevier.
- Ooki, A., Nomura, D., Nishino, S., Kikuchi, T., & Yokouchi, Y. (2015). A global-scale map of isoprene and volatile organic iodine in surface seawater of the arctic, northwest pacific, indian, and southern oceans. *Journal of Geophysical Research: Oceans*, 120(6), 4108–4128. doi: <https://doi.org/10.1002/2014JC010519>
- Wohl, C., Brown, I., Kitidis, V., Jones, A. E., Sturges, W. T., Nightingale, P. D., & Yang, M. (2020). Underway seawater and atmospheric measurements of volatile organic compounds in the southern ocean. *Biogeosciences Discussions*, 2020, 1–40. Retrieved from <https://www.biogeosciences-discuss.net/bg-2020-2/> doi: 10.5194/bg-2020-2

**Table S1.** Surface (0 – 10 m) isoprene concentration measurements (pM) in the SO (>40°S) used for ISOREMS model development. \*GC-MS: Gas Chromatography Mass Spectrometry. \*\*PTR-MS: Proton Transfer Reaction - Mass Spectrometry.

Mean [Min – Max]	Southern Ocean Area	Cruise name	Method	Source
10.7 [2.1 – 88.4]	Southern Ocean Circumnavigation	ACE	GC-MS*	This work
22.4 [1.6 – 93.5]	Atlantic sector and Weddell Sea	ACE	GC-MS*	This work
29.1 [13.2 – 57.1]	Atlantic sector	AMT22 & AMT23	GC-MS*	Hackenberg et al. (2017)
9.5 [2.3 – 39.0]	Indian sector	KH-09-5	GCMS*	Ooki, Nomura, Nishino, Kikuchi, and Yokouchi (2015)
13.5 [4.8 – 39.1]	Atlantic sector	ANDREXII	PTR-MS**	Wohl et al. (2020)

**Table S2.** Variables used in this work and their sources.

Abbreviation	Name	Source	Units	% matchup	Mean [Minx – Max]	Reprocessing status
ISO	Isoprene concentration	Table S1	pM	–	14.6 [1.0 – 93.5]	–
CHL	Chlorophyll-a concentration	MODIS aqua	$\mu\text{g L}^{-1}$	86.84	0.45 [0.07 – 3.20]	R2018.0
SST	Sea surface temperature	MODIS aqua	Deg. C	84.65	3.02 [-1.80 – 12.30]	R2014.0
PIC	Particulate Inorganic Carbon	MODIS aqua	Mol m-3	86.84	$4.17 \times 10^{-4}$ [ $1.19 \times 10^{-5}$ - $2.5 \times 10^{-3}$ ]	R2018.0
PAR	Photosynthetically Active Radiation	MODIS aqua	$\text{Einstein m}^{-2} \text{d}^{-1}$	96.93	33.62 [8.81 – 66.49]	R2018.0
POC	Particulate Organic Carbon	MODIS aqua	$\text{mg m}^{-3}$	86.40	91.85 [33.65 – 254.04]	R2018.0
ZEU	Depth of the Euphotic Layer	MODIS aqua	m	93.86	57.54 [17.71 – 112.32]	R2018.0
MLD	Mixing Layer Depth	Holte, Talley, Gilson, and Roemmich (2017)	m	100	38.43 [10.98 – 145.72]	R2018.0

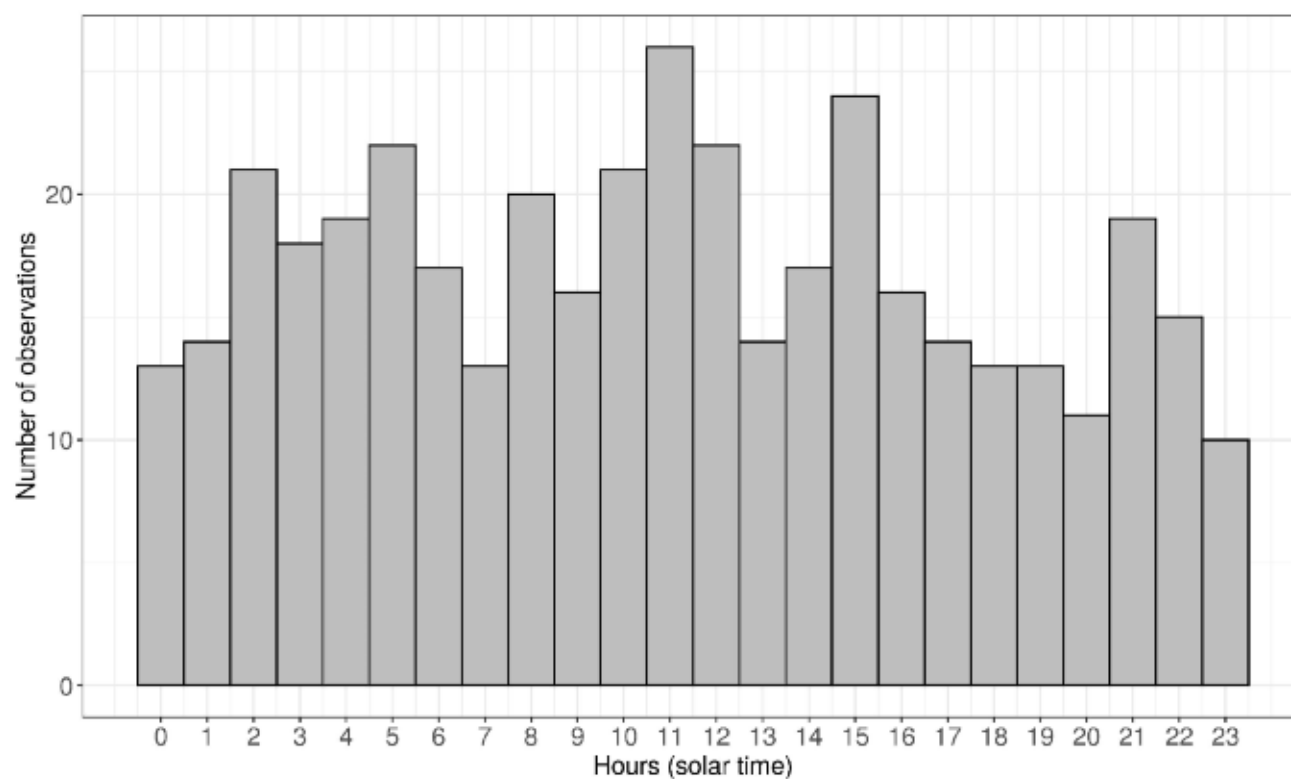


**Figure S1.** Number of isoprene concentration measurements over the diel cycle of solar times.

Solar times were calculated from GMT time and longitude using the *solaR* package on R.

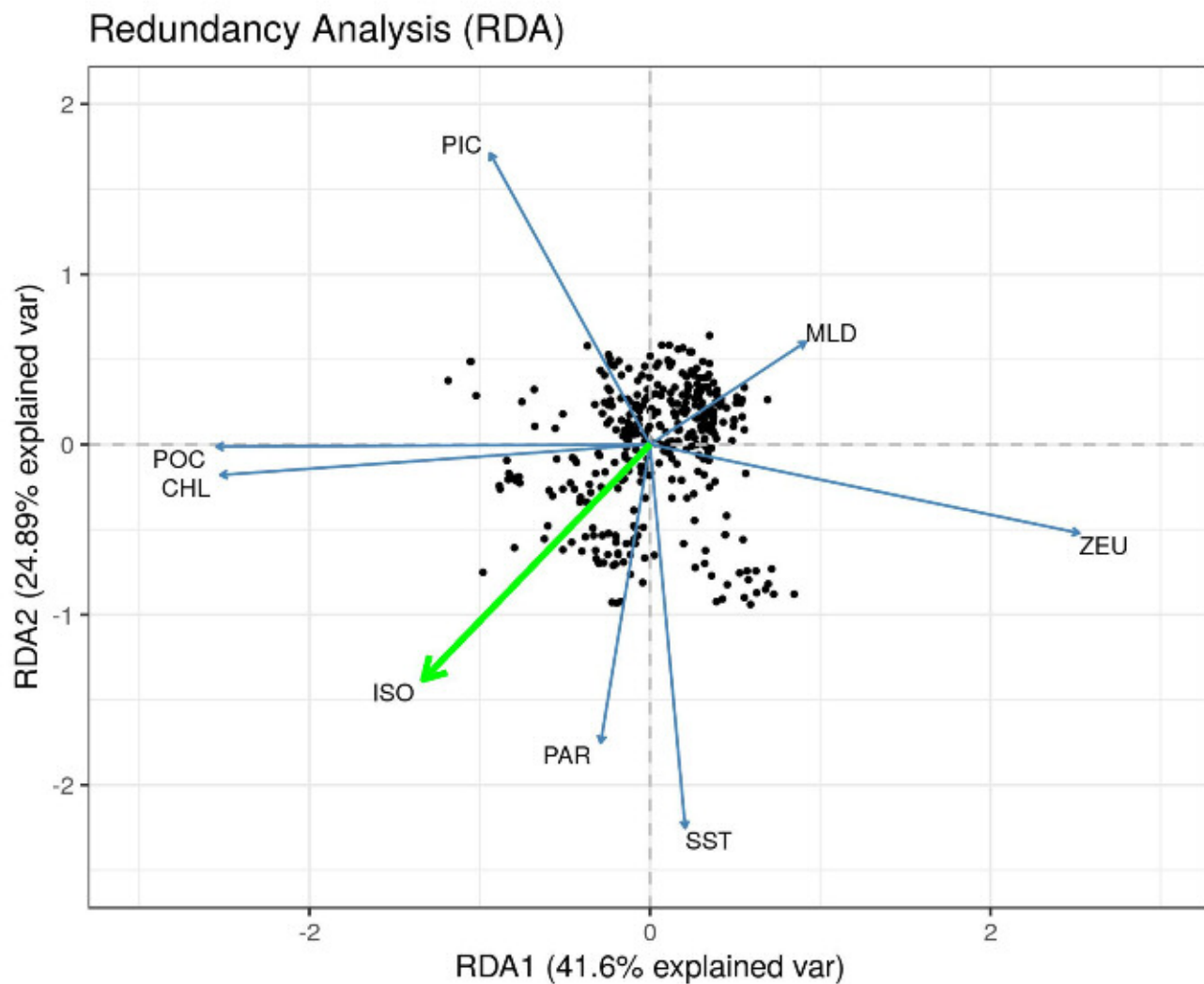


**Figure S2.** Redundancy analysis (RDA) (Legendre & Legendre, 2012) of isoprene concentration and remote sensing variables using *vegan* package on R. After checking the non-normality distribution of our variables using Shapiro-Wilks test, data were log-transformed. See Table S2 for abbreviations.

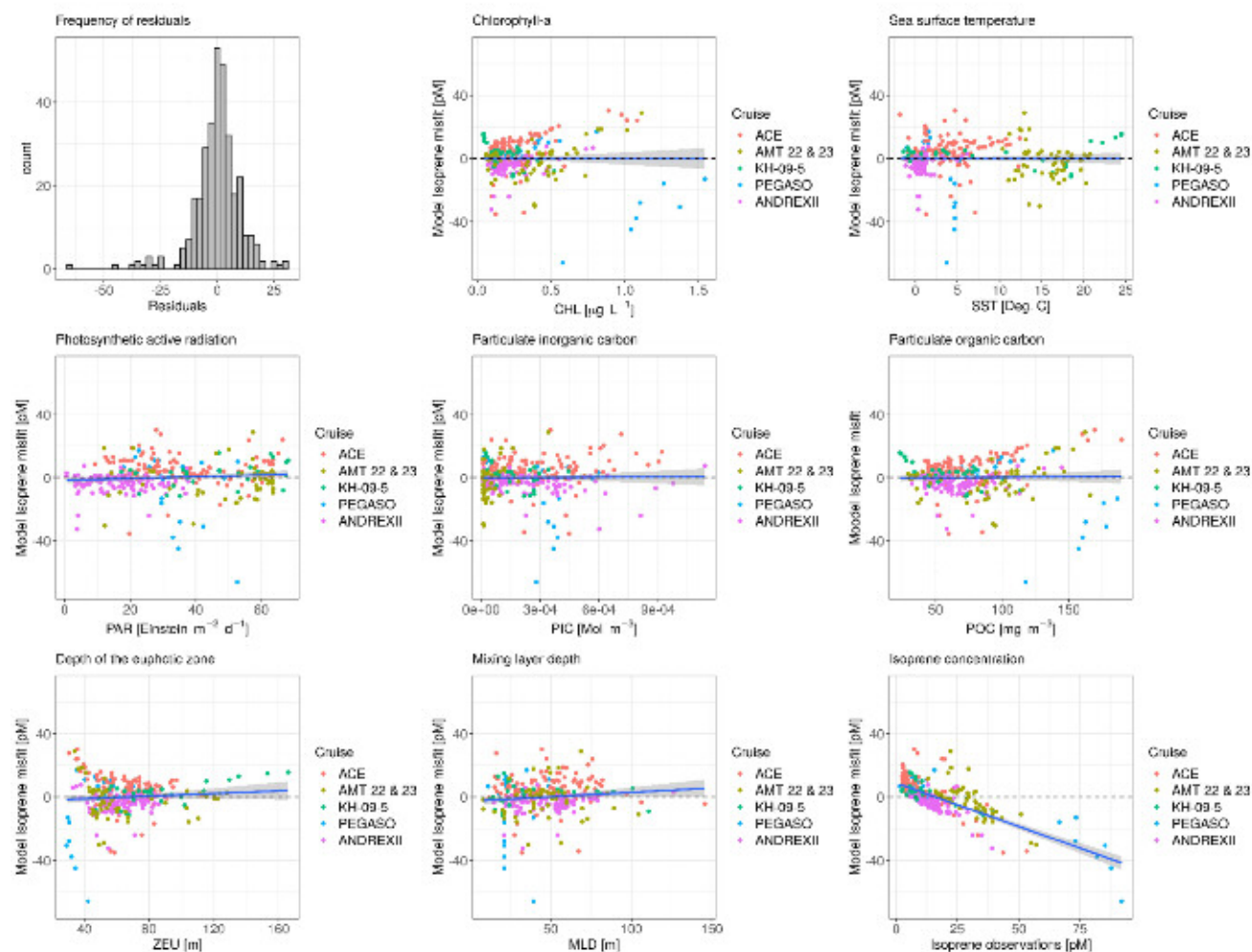


**Figure S3.** First panel: Scatter plot of ISOREMS predictions vs. observations of isoprene concentrations. Other panels: Misfit (residuals) of ISOREMS-predictions vs. each of the potential predictive variables tested (ISO, CHL, SST, PIC, PAR, POC, ZEU, MLD; Table S2). Last panel: Misfit of ISOREMS-predictions vs. observed isoprene concentrations.

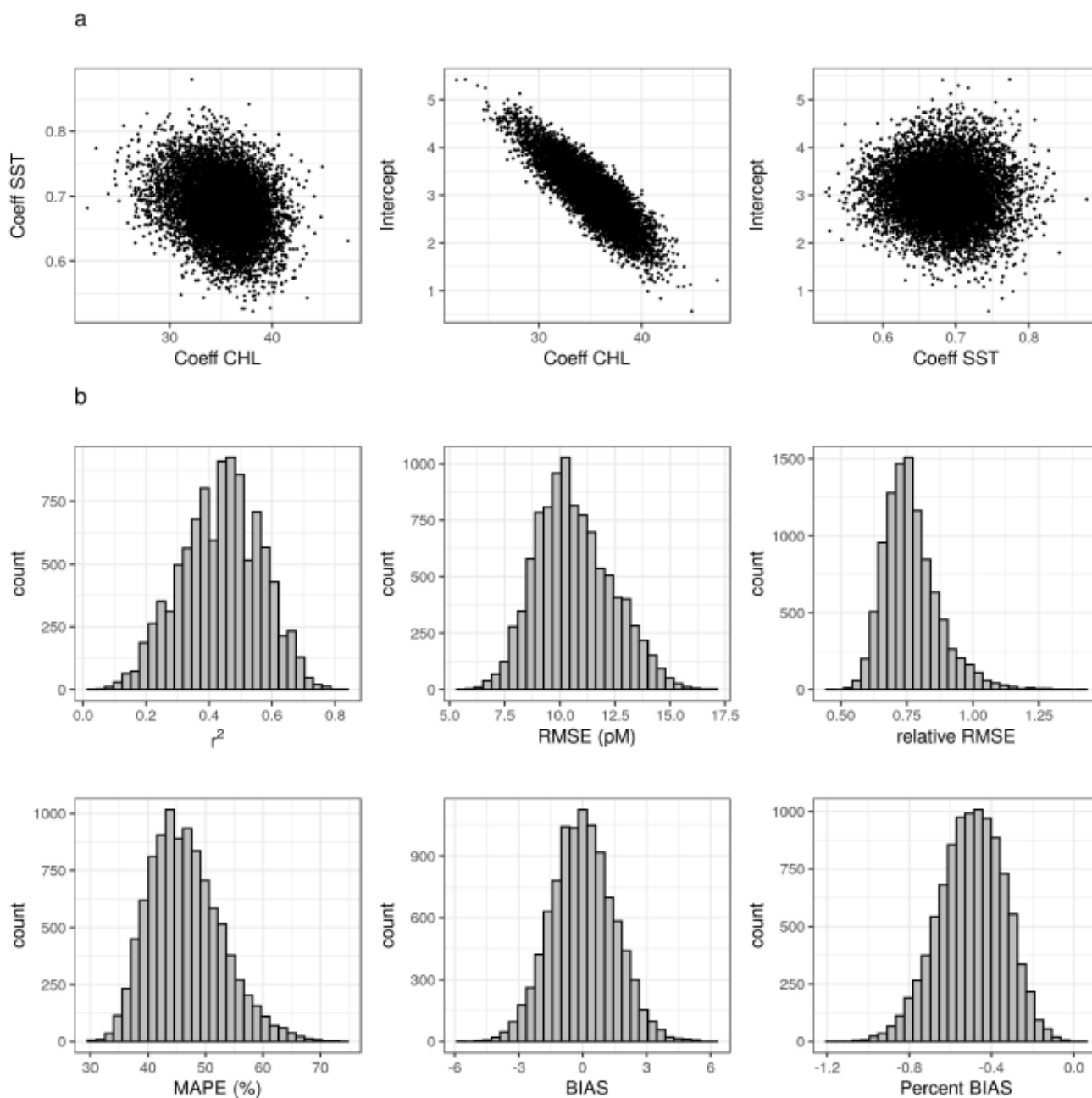


**Figure S4.** (a) Scatter-plot of the coefficients of CHL and SST and the intercepts of the multiple linear regressions of random-sampling (80%) simulations (see text for details). (b) Histograms of the validation statistics ( $r^2$ , RMSE, relative RMSE, BIAS, percent BIAS, and MAPE) randomly generated by the above simulations on 20% of the data. Number of simulations = 10,000.

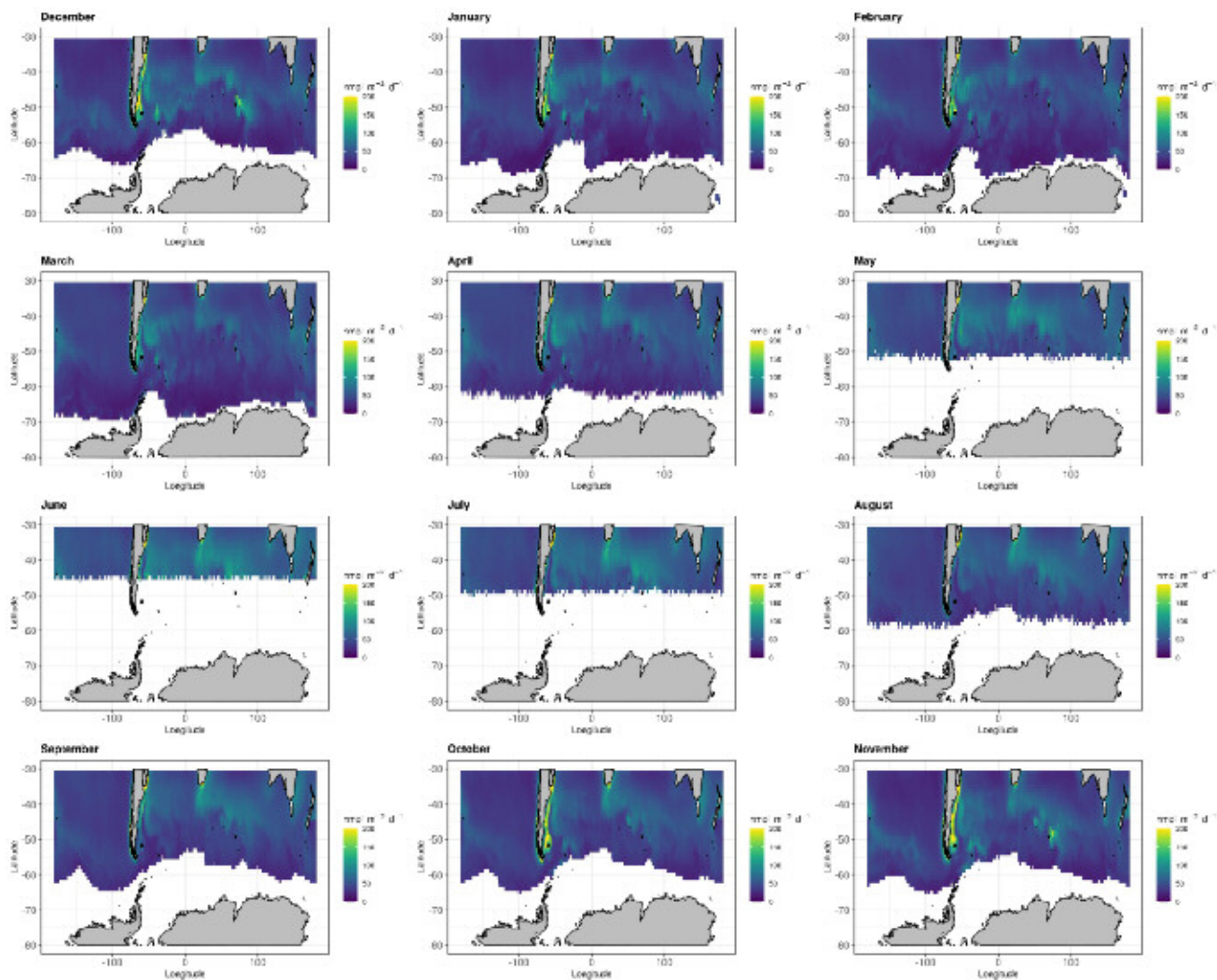


**Figure S5.** Monthly climatology of  $ISO_{ISO\ REMS}$  emission fluxes in the Southern Ocean. Blank spaces are pixels where either satellite CHL or wind speed are lacking.